Adsorption (2009) 15: 227–239
DOI 10.1007/s10450-009-9171-z

Functionalized hexagonal mesoporous silica monoliths with hydrophobic azo-chromophore for enhanced Co(II) ion monitoring

Sherif A. El-Safty

Published online: 17 April 2009

Abstract We introduce here new optical strips for the colorimetric monitoring of Co(II) ions in an aqueous solution. The optical nanosensors were designed by direct immobilizing azo-chromophore with long hydrophobic tails onto hexagonal mesoporous silica monoliths (HOM-2). Although, azo-dye probe was used as signaling reporter for selective detection of the Co(II) analyte up to 10^{-6} mol/dm^3 in solution, the tailoring of the Co(II) ion-sensing functionality was successfully manipulated up to 10^{-9} mol/dm^3 with the incorporation of azo-chromophore into hexagonal mesoporous silica monoliths (HOM-2), which led to small, easy-to-use optical sensor strips. However, our simple design of colorimetric sensors is based on a physical adsorption of chemically responsive dyes onto HOM materials followed by stronger dye-analyte interactions in aqueous sensing systems. No elution of the probe molecules was evident with the addition of Co(II) analyte ions during the sensing process. The binding of Co(II) ions with probes led to the color change of nanosensors corresponding to the formation of the metal-chelate [Co(II)-Probe]$^{n+}$ complexes. Results indicated that hexagonal nanosensors offer one-step and simple sensing procedures for both quantification and visual detection of Co(II) ions without the need for sophisticated instruments. However, the solid HOM-2 materials immobilized by the these indicator dyes, in principle, could be used as preconcentrators to yield high adsorption capacity and preconcentration efficiency, leading to simultaneously visual inspection and simple detection over a wide, adjustable range of Co(II) ions even at trace levels. For Co(II) ion selectivity assays, negligible changes in either the developed color or the reflectance intensities of the [Co-Probe]$^{n+}$ complex were observed, despite the addition of competitive cations. Moreover, the hexagonal nanosensors are reversible and have the efficient potential to serve for multiple analyses.

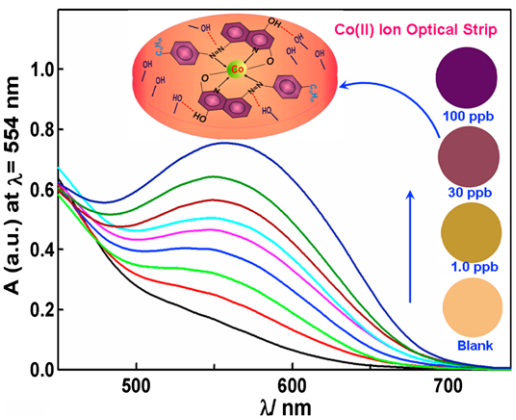

Hexagonal optical strips for the colorimetric monitoring of Co(II) ions in an aqueous solution was successfully fabricated. This strip enabled to create ion-sensitive responses with revisable, selective and sensitive recognitions of a wide range of detectable Co(II) ions down to sub-nanomolar ($\sim 15 \times 10^{-9}$ M) in rapid sensing responses (in the order of minutes)

Keywords Co(II) ions · Detection · Optical sensor · Hexagonal monoliths · Azo-chromophore

This special Festschrift for Professor Jaroniec.

S.A. El-Safty (✉)
Materials Interdisciplinary Group, Innovative Materials Engineering Laboratory, National Institute for Materials Science (NIMS), Sengen 1-2-1, Tsukuba, Ibaraki 305-0047, Japan
e-mail: sherif.elsafty@nims.go.jp

1 Introduction

Interest in the biological and environmental monitoring of heavy metals has increased during the last decades (Simpson 2000; Dominique 2007). The reason is that large amounts of toxic and carcinogenic metals have been released into the environment, especially in industrial areas (Keith et al. 2007; Buhlmann et al. 1998; Pretsch et al. 1997). Environmental exposure to these toxic elements may lead to both short-term and long-term health risks. Cobalt is a trace element found in the environment. Cobalt contents in various foodstuffs have been complied (Hamilton 1994). Humans may be exposed to cobalt compounds from diet and from occupational exposure in several industries such as hard metal industry, diamond polishing, and the porcelain, chemical and pharmaceutical industries (Christensen and Poulsen 1994). The daily intake of cobalt from food has been estimated to be between 5–45 μg/day mainly from vegetables, meat and pluck (Alexandersson 1988). Cobalt exposure may result in adverse health effects such as asthma, contact dermatitis, myocardiopathy and several impaired lung function, depending on exposure levels (Haga et al. 1996; Angerer et al. 1989; Hartung et al. 1982). The FAO (Food and Agriculture Organization of United Nations) and WHO (World Health Organization) have recommended a 2.4 μg/day of vitamin B12 (equivalent to 0.1 μg/day of cobalt to the adult diet. Recently, cobalt and its compounds were classified as possible human carcinogens (Elinder 1984; Nagpal 2004). The most famous example of Co(II) ion toxicity in man occurred in Europe and North America in 1960s when cobalt sulfate was added to beer as a form of foam stabilizer (Imray and Landley 1999), which produced severe cardiomyopathy, haematologic, neurologic and thyroid abnormalities (Morgan 1983; Jensen and Tüchsen 1990). Several reports have described cobalt-related asthma and contact dermatitis from cobalt as problems of considerable magnitude (Mennè and Nieboer 1989). Overall, the discharge of cobalt into the environment can cause neurotoxicological disorders and genotoxicity in human beings and in chronic cases can even cause cancer (Lison et al. 2001; Pal et al. 2006). The data relating to genotoxicity and carcinogenicity of cobalt have been reviewed (De Boeck et al. 2003).

Since systematic efforts and triggering of allergic, and carcinogenic diseases may occur at cobalt exposure levels of few μmol, eliminating humans from cobalt exposures and providing a generic approach to risk assessment, which focused on human health and the wider environment have been a long standing research attraction in the environmental pollution monitoring (Hursthouse 2001). Methods capable to quantify trace cobalt ions at low level include atomic absorption spectroscopy (AAS), inductively coupled plasma (ICP) combined with atomic emission spectroscopy (ICP-AES) or with mass spectroscopy (ICP-MS), electrochemical and potentiometric techniques, X-ray fluorescence, and molecular absorption spectroscopy are being powerful methods owing to their multielement capacity and high sensitivity (Dadfarnia and Jafarzadeh 1999; Burns and Kheawpinting 1984; Safavi and Shams 2000; Vega and Van der Berg 1997; Benkhadda et al. 2000; Singh et al. 2007). The majority of these methods, however, are not used for routine applications (Wolfbeis 2005). In addition, careful planning and testing are often required with these analytical protocols, leading to many handling steps with sample preparation to alleviate sample matrix interferences (Anastas 1999). As a result, a low-cost, easy-to-use, and reliable device is still much needed for environmental monitoring and green chemistry (Niessner 1991; Oehme and Wolfbeis 1997).

Among the many analytical techniques, optical sensor of toxic trace element measurements was efficiently used to detect pollutant species with large economic, political and social impact (Wolfbeis 2005). Basically, the chemical sensors are molecular receptors that transform their chemical information into analytically useful signals upon binding to specific guests. This visual inspection approach is advantageous because it involves simple techniques that have fairly few handling steps and do not require sophisticated equipments (Nam et al. 2003; Zhang and Suslick 2005). In optical chemical sensing, color changes of chromophore receptors are induced via nonspecific interaction with ion analyte species, indicating significant signaling and selective response to the analytes. Recognizing that humans are visual creatures and that our imaging technology is highly advanced yet inexpensive (El-Safty et al. 2006; Carringto and Xue 2007). The key components in this sensing method are optical sensors that are highly stable and can efficiently detect toxic ions in terms of sensitivity and selectivity with real-time monitoring; such features are currently required to analyze today's ultra-trace levels of environmental pollutants (Lee et al. 2007; Umemura et al. 2006; Ros-Lis et al. 2005). Optical sensors for Co(II) ion detection have successfully emerged using chromophores- and fluorophores-functionalized polymers (Yang et al. 2002; Malcik et al. 1998) but they were normally associated with certain limitations such as, tedious synthesis, complicated analysis, delayed signal response, insufficient selectivity and low sensitivity.

Recently, nanometer-sized materials with engineered features, including size, shape, composition, and function play a leading role for their emerging applications in optical detection of cations and anions (El-Safty et al. 2007a, 2007b, 2008a, 2008b, 2008c; Comes et al. 2004; Desacalzo et al. 2005). In fact, ordered mesoporous silica monoliths that have a uniformly-sized, monodispersed porosity in the range of 2–20 nm, and a large particle size show promise of a new class of optical sensor materials. In such systematic sensor

design, the anchoring of organic dyes into 3D inorganic networks with well-defined cage cavities enhanced the sensitivity of toxic analytes (El-Safty et al. 2007a, 2007b). The large particle size of monoliths, however, led to the creation of pore surface grains (macroscale length) that enabled grafting of a large number of probe binding sites to the pore wall surfaces of silica matrices. Although, these successful designs of nanosensors allowed us to controlled assessment processes with naked-eye detection of several toxic heavy metal ions up to nanomolar concentrations (El-Safty et al. 2008a, 2008b, 2008c), challenges to make smart detection eco-friendly solid sensors for Co(II) ions in the basic laboratory assays still in demand. The use of the solid optical sensor in a powder form led to constrain use as sensory optical devices. Ideal sensory systems with small molecule-based sensor strips remain an attractive approach. In this regard, important development has been recently reported to use the 3D nanoscale monolithic discs as chromophore platforms enabled sensitive recognition of metal ions up to sub-picomolar detection limits ($\sim 10^{-11}$ mol/dm^3), for first time, with rapid response time within few seconds (El-Safty et al. 2008a, 2008b, 2008c).

Here, we reveal a real evidence of the design of hexagonal optical strips for the colorimetric monitoring of Co(II) ions. Direct immobilization of a chemically synthesized azo-dye chromoionophore onto hexagonal HOM-2 monolithic materials led to fabricate optical nanosensors. These hexagonal nanosenor strips enabled to create Co(II) ion-sensing system responses with revisable, selective and sensitive recognition up to 10^{-9} mol/dm^3, leading to small, easy-to-use optical sensor strips. The key result in our study is that the hexagonal nanosensor design exhibited significant Co(II) ion-selective ability of these target ions from environmental samples and waste disposals.

2 Experiments

2.1 Chemicals

All materials were used as produced without further purification. N-alkyl-oligo(ethylene oxide), and Triton X-100 surfactants, and tetramethylorthosilicate (TMOS), which was used as the silica source, were obtained from Sigma-Aldrich Company Ltd., USA. The polyoxyethylene(10)-stearyl ether (***Brij76***, $C_{18}H_{37}(OCH_2CH_2)_{10}OH$, M.av = 711) was obtained from Wako Pure Chemicals Ltd., Osaka, Japan. For the synthesis of azo-chromoionophore, 4-dodecyl aniline, nitrous acid and sodium nitrite were purchased from Aldrich Chem. Co., USA. 2,4-quinolinediol was procured from Tokyo-Kaisei Kogyo Company. Ltd., Japan. Standard cobalt (Co^{2+}) and other metal ion concentrations were prepared from their corresponding AAS grade (1000 μg/mL) solutions. These stock solutions were procured from Wako Pure Chemicals, Japan. For pH adjustments, buffer solutions (0.2 M) of KCl-HCl, CH_3COOH-CH_3COONa, 3-morpholinopropane sulfonic acid (MOPS)-NaOH, 2-(cyclohexylamino) ethane sulfonic acid (CHES)-NaOH, and N-cyclohexyl-3-aminopropane sulfonic acid (CAPS)-NaOH were used. The MOPS, CHES and CAPS were procured from Dojindo Chemicals, Japan, and the remaining from Wako Pure Chemicals, Japan.

2.2 Synthesis of the 8-(4-n-dodecyl-phenylazo), 2,4-quinolinediol (azo-chromoionophore)

The azo-chromoionophore was prepared by dissolving 4-dodecyl aniline (26 g, 0.1 mol) in 50 ml solution of 0.2 M H_2SO_4, for 1 h stirred at 0–2 °C. To this homogeneous mixture, an ice-chilled 50 mL solution of sodium nitrite (6.8 g, 0.1 mol) was added drop-wise, followed by vigorously stirred for 2 h, under freezing conditions. The excess nitrous acid was quenched with urea, and an equivalent quantity of 2,4-quinolinediol (14.5 g, 0.1 mol), dissolved in 50 ml of NaOH (0.25%) was added to the diazotate at 1–3 °C. The reaction mixture for overnight stirring and the desired product was obtained as a brownish orange precipitate. The solid product was filtered and purified by washing with hot and cold water. The purity of the product was analyzed by CHNS elemental analyses as follows: **CHN**: **C**, 74.64; **H**, 8.29; **N**, 9.6, as consistent with $\mathbf{C_{27}H_{36}N_3O_2}$ molecular formula, which required **C**, 74.65; **H**, 8.295; **N**, 9.67%. **UV-Vis** (Medium: 75% EtOH): λ_{max} 395 nm, ε 2.37×10^4 dm^3 mol^{-1} cm^{-1} (Qu denotes quinolinediol). Moreover, the azo-probe were analyzed by using ^{1}H and ^{13}C NMR spectroscopy. The data were as follows: **^{1}H NMR** (400 MHz, $CDCl_3$) : δ 0.89 (t, $J = 7.0$ Hz, 3H, CH_3), 1.3–1.53 (m, 16H, 8xCH_2), 1.9 (p, $J = 7.2$ Hz, 2H, CH_2), 2.83 (t, $J = 7.6$ Hz, 2H, CH_2), 8.94 (d, $J = 8.8$ Hz, 1H, QuH), 8.5 (d, 1H, QuH), 8.3 (d, 1H, QuH), 8.2 (d, 1H, QuH), 7.25 (d, 1H, ArH), 7.35 (d, 1H, ArH), 6.81 (d, 1H, ArH), 5.29 (s(b), 2H, Qu-OH); **^{13}C NMR** (100 MHz, $CDCl_3$): δ 14.5 (CH_3), 22.9 (CH_2), 29.6 (CH_2), 29.7 (CH_2), 29.8 (CH_2), 29.8 (CH_2), 29.6 (CH_2), 29.3 (CH_2), 29.2 (CH_2), 29.7 (CH_2), 29.8 (CH_2), 32.1 (CH_2), 166.1 (Qu, C), 145.7 (Qu, CH), 140.1 (Qu, CH), 122.1 (Qu, CH), 124.1 (Qu, CH), 106.1 (C), 125.1 (CH), 137.1 (CH), 167.41 (Qu, C-OH), 178.9 (Qu, C-OH).

2.3 Synthesis of hexagonal monoliths (HOM-2) as probe carriers

HOM-2 silica monoliths were synthesized by using direct templating method of lyotropic liquid crystalline phase of Brij76 as template, as previously reported (El-Safty and Evans 2002). In typical conditions, the composition mass

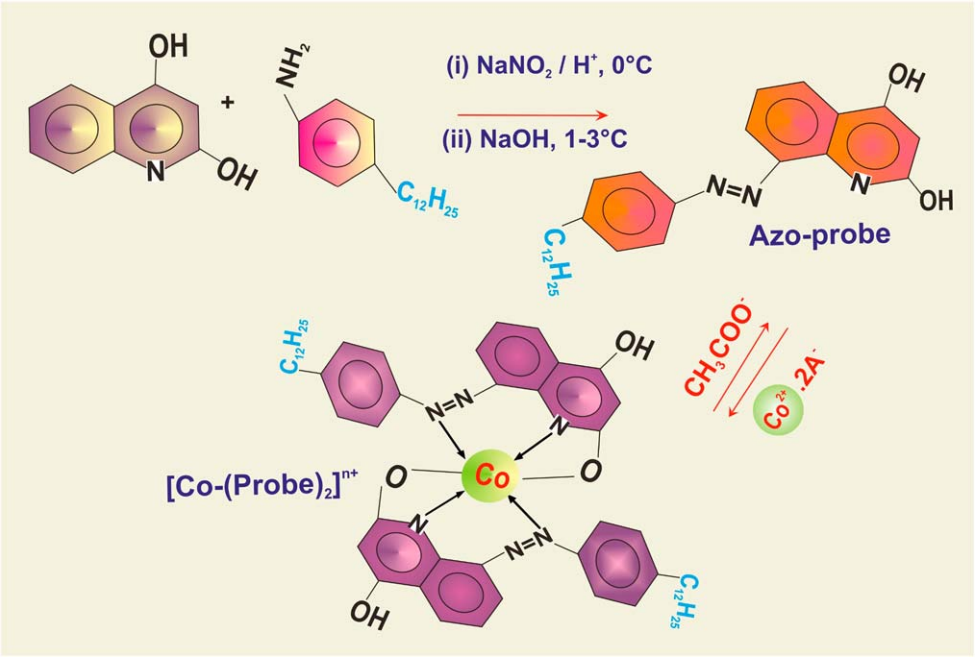

Scheme 1 Synthesis of 8-(4-n-dodecyl-phenylazo), 2,4-quinolinediol (**azo-probe**) and the reversible complex formation during the recognition of Co^{II} ions in solutions at temperature 25 °C, volume 25 ml and pH 5.5, respectively

ratio of Brij76:TMOS:HCl/H_2O was 1:2:1 respectively. Homogeneous sol-gel synthesis was achieved by mixing Brij76/TMOS in a 100-cm^3 beaker and then shaking at 50 °C for 2 min until homogeneous. The exothermic hydrolysis and condensation of TMOS occurred rapidly by addition of acidified aqueous solution of HCl (at pH = 1.3) to this homogeneous solution. The resulting an optical gel-like material was put in a graduate ingot and acquired the shape and size of the cylindrical casting vessel. To obtain centimeter-sized, crack-free, and disc-like silica translucent membranes, the materials were gently dried at room temperature for 3 hours and then allowed to stand in a closed ingot for 1 day to complete the drying process. After calcination at 450 °C for 6 h under normal atmosphere, the transparency of the disc-like membranes was lost due to the microcracking within the silica matrix, while their macroscopic shapes with high dimensional stability, rigidity (with stress 10 hPa), and porosity were retained (El-Safty and Hanaoka 2003; El-Safty et al. 2005).

2.4 Fabrication of hexagonal sensor strips

Direct incorporation of hydrophobic azo-chromophore molecules onto the hexagonal HOM-2 monoliths (thickness 0.05 cm; diameter 1.02 cm; volume 2.5×10^{-5} dm^{-3}) was adapted for the fabrication of nanosensor strip (see Scheme 2). The azo-probe (0.05 mmol) was dissolved in dehydrated ethanol and equilibrated with HOM-2 monoliths for 2 h at 20 °C. The impregnation procedure was performed under vacuum at 25 °C to reach probe saturation. The probe anchored HOM-2 membranes were washed with deionized water and dried at 60 °C for 45 minutes.

2.5 Recognition procedure for Co(II) ions

In a typical sensing experiment, a mixture containing specific concentrations of toxic Co(II) ions adjusted at pH solution of 5.5 by using MOPS for the sensor. This Co(II) analyte mixture was directly added to the monolithic sensors at constant volume (20 cm^3) with shaking at room temperature. Studies on the sample volume also indicated that the volume at 20 cm^3 was sufficient for effective interaction of Co^{2+} with sensor strip to give good color separation (El-Safty et al. 2008a, 2008b). A blank solution was also prepared, following the same procedure for comparison. After an interval time of (5–15 min), the monolithic sensors were filtered after equilibration time, according to the feature of Co(II) ion-sensors (Scheme 2), using cellulose acetate filter paper (25 mm; Sibata filter holder) and used for visual color assessment and absorbance measurements. In a typical experiment, the Co(II) ion-sensing system was studies by batch equilibration method at various pH values. The concentrations of toxic Co(II) ions were calculated by comparing the colour intensity of the target samples with that of the standard samples, which were prepared with known concentrations of analyte solutions.

2.6 Analyses

Small-angle powder X-ray diffraction (XRD) patterns were measured by using an MXP 18 diffractometer (Mac Science Co. Ltd.) with monochromated CuKα radiation with scattering reflections recorded for 2θ angles between 0.3° and 6.5° corresponding to d-spacings between 29.4 and 1.35 nm. N_2 adsorption-desorption isotherms were measured using a

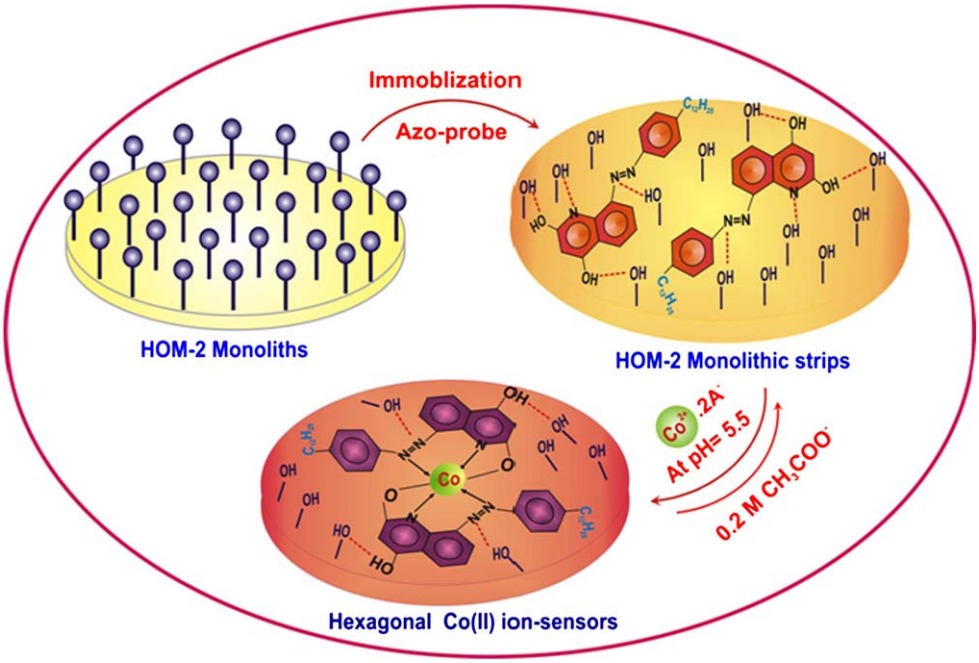

Scheme 2 Representative design of the hexagonal strip by direct constructing the azo-probe with possible interactions into hexagonal HOM-2 monolithic disc and the optical signaling responses of the nanosensor for Co(II) ion with the formation of the $[Co\text{-}(probe)_2]^{n+}$ complex, and the reversible process by using 0.2 M CH_3COOH solution for several times

BELSORP36 analyzer (JP. BEL Co. Ltd.) at 77 K. The pore size distribution was then determined from the adsorption curve of the isotherms by using nonlocal density functional theory (NLDFT). Transmission electron microscopy (TEM) was obtained by using a JEOL TEM (JEM-2000EXII) operated at 200 kV with a side-mounted CCD Camera (Mega View III from Soft Imaging System Co.). The TEM samples were prepared by dispersing the powder particles onto holey carbon film on copper grids. Thermogravimetric and differential thermal analyses (TG and DTA, respectively) were done using a Thermo Plus TG8120 (Rigaku, Japan). X-ray photoelectron spectroscopy (XPS) was obtained by using a PHI Model 5600 Multi-Technique systems (Perkin-Elmer Co., USA) with monochromated AlKα radiation. Energy Dispersive X-ray microanalysis (EDS-130S) was used to determine the elemental compositions of the azo-probe functionalized HOM-2 carriers. ^1H and ^{13}C NMR spectra at room temperature for azo-probe were also measured using a Varian 400-MR model (Varian Inc., USA) with software VNMR 6.1C version operated at 500 and 125 MHz for ^1H and ^{13}C NMR spectrometer. We used $CDCl_3$ as a solvent. The absorbance spectrum of the sensor material was recorded using a Shimadzu 3150 model solid-state UV-Vis spectrophotometer. The metal ion concentration after equilibration was determined with a Seiko SPS-1500 model inductively coupled plasma atomic emission spectrometer (ICP-AES). Buffer solutions were adjusted to ambient pH values using a Horiba F-24 (Kyoto, Japan) model microcomputerized pH/Ion meter.

3 Results and discussion

3.1 Characterization of hexagonal monolithic nanosensor

The most common method used for design of optical chemical sensor arrays is the grafting technique (El-Safty et al. 2006; Carrington and Xue 2007). In this current design, the optical azo-probe nanosensor was fabricated via direct inclusion of ethanol solution of azo-probe into hexagonal HOM-2 monoliths without use of surface modifiers such as silane- or thiol-coupling agents. However, the removal of ethanol by vacuo at ambient temperature led to create sufficiently physisorbed "short-range" interactions (i.e. van der Waals and H-bonding interactions) between the abundant hydroxyl groups of pore surface silicates and the heteroatoms of azo-probe molecules (Scheme 2). In addition, the long alkyl chains ($\geq C_{12}$) of the modified-probe molecules offer the required hydrophobicity to prevent the leaching of the probe receptors from HOM-2 monoliths during the detection of Co(II) ion in aqueous solutions. Such interactions are necessary to achieve retention of the azo-probe modified monoliths during the washing cycle and potential sensing recognition of Co(II) ions. Although, the binding events of the Co(II) ion with hydrophobic azo-probe might lead to increase the hydrophilicity of the probe molecules, no evidence of the probe leaching in aqueous phase was distinctive during the Co(II)-probe complexation (Scheme 2).

Compared with our preliminary design of chemosensors using surface modifications (El-Safty et al. 2006, 2007a, 2007b), in which expensive reagents of thiol- or silane-coupling agents were used to tune the polarity of the porous silica surfaces prior to the immobilization of chromophores,

our optical chemosensor design here was successfully fabricated without such coupling agents, indicating the low operating cost system. Moreover, this direct inclusion of the azo-probe might achieve higher flexibility on the specific activity of the electron acceptor/donor strength of the molecular probe than that immobilization method using surface modifiers. Although, the surface modification method enhanced the stability of the sensor due to strong electrostatic interactions 'Coulombic-types' between the probe molecule and charged silica surfaces, limitations in the electron mobility of the functional site of the receptors might be occurred (El-Safty et al. 2007a, 2007b). Thus, the direct inclusion approach led to high accessibility of the binding site of the probes, in which easily generate and transduce an optical color signal and a fast kinetic azo probe-Co(II) binding responses were evident.

The amount (Q) of azo-probe immobilized HOM-2 at saturation was calculated by (1) (El-Safty 2003):

$$Q = (C_0 - C_t)V/m \quad \text{(mmol/g)} \tag{1}$$

where Q_t is the adsorbed amount at contact time t, V is the solution volume (L), m is the mass of HOM carriers (g), C_0 and C_t are the initial concentration and the concentration at saturation time, respectively (see Table 1). Despite such simple procedure for design of nanosensors, the high loading capacity (Q) of the probe was attributed to the hexagonal nanoscale pore ordering and large particle size characteristics of the monolithic disc (El-Safty et al. 2007a, 2007b). The loading capacity of the azo-probe onto HOM-2 monoliths was also revealed based on TG-DTA techniques (Fig. 1). The TG profile shows the gradual decrease in the weight of the monolithic strips up to 12 wt% from 25–900 °C. The TG curve indicates three distinct stages of weight loss accompanied by a DTA exothermic peak in each of the three stages. First, the weight loss of 2.5 wt% before 250 °C might indicate the evaporation of physically adsorbed H_2O and remained ethanol with probe-HOM-2 sensor. Second, the weight decrease between 250 and 700 °C is related to azo-probe decomposition, which corresponds to the strong exothermic DTA peaks around 250–650 °C. Thus, the weight loss of 10 wt% between 250 and 650 °C might be attributed to the decomposition of azo-probe, coinciding with the adsorption amount (Q) of the loaded azo-probe moieties of these materials (Table 1). Third, the further weight loss after 650 °C might be assigned the further condensation of the silica species. These results from the TG analyses were consistent with elemental content results from EDS X-ray microanalysis of C, H, N, and S. Based on elemental analyses, the composition of CHNS with azo-probe modified HOM-2 monoliths was 9.8 mass%.

The XRD pattern (Fig. 2) of hexagonal HOM-2 disc and strip showed different peaks, respectively assigned to d-spacing ratios of $1:1/\sqrt{3}:1/\sqrt{4}$, indicating the retention of long-range ordered hexagonal lattices (El-Safty and Evans 2002). The diffraction intensity and the hexagonal d_{100}-value of both materials were significantly unchanged (Fig. 2A). The N_2 isotherms show that typical type IV adsorption behavior with a well-known sharp inflection of adsorption/desorption branches was featured the materials (Fig. 2B). The adsorption branches were significantly shifted toward lower relative pressure (P/P_0) with embedding the azo-probe into HOM-2 disc, indicating the inclu-

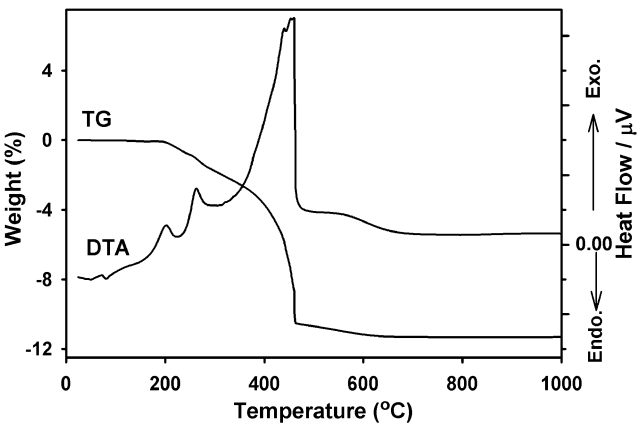

Figure 1 TG and DTA analyses of azo-probe functionalized hexagonal membrane sensor

Table 1 Tolerance concentration for interfering matrix species during recognition of [3.0 ppm] Co(II) ions in solution by azo-dye receptor

Tolerance limit for common electrolyte species (ppm) in solution											
NaCl	NaBr	KNO_3	SO_4^{2-}	F^-	PO_4^{3-}	CO_3^{2-}	NO^{2-}	ClO_4^-	IO_3^-	SCN^-	SO_3^{2-}
1380	1100	1010	2000	150	170	230	210	180	20	20	185
Tolerance limit for foreign cations (ppm) in solution											
Sn^{2+}	Fe^{3+}	Mn^{2+}	Hg^{2+}	Ni^{2+}	Zn^{2+}	Cu^{2+}	Ir^{3+}	Cr^{6+}	Sb^{3+}	Al^{3+}	Bi^{3+}
1.8	1.6[b]	2.0[a]	1.0[a]	0.65[a]	0.8[a]	0.6[a]	2.3	1.6	2.0	2.0	2.0

[a]Data obtained after using suppressing agents

[b]Eliminated using 0.2 mM pyrophosphate

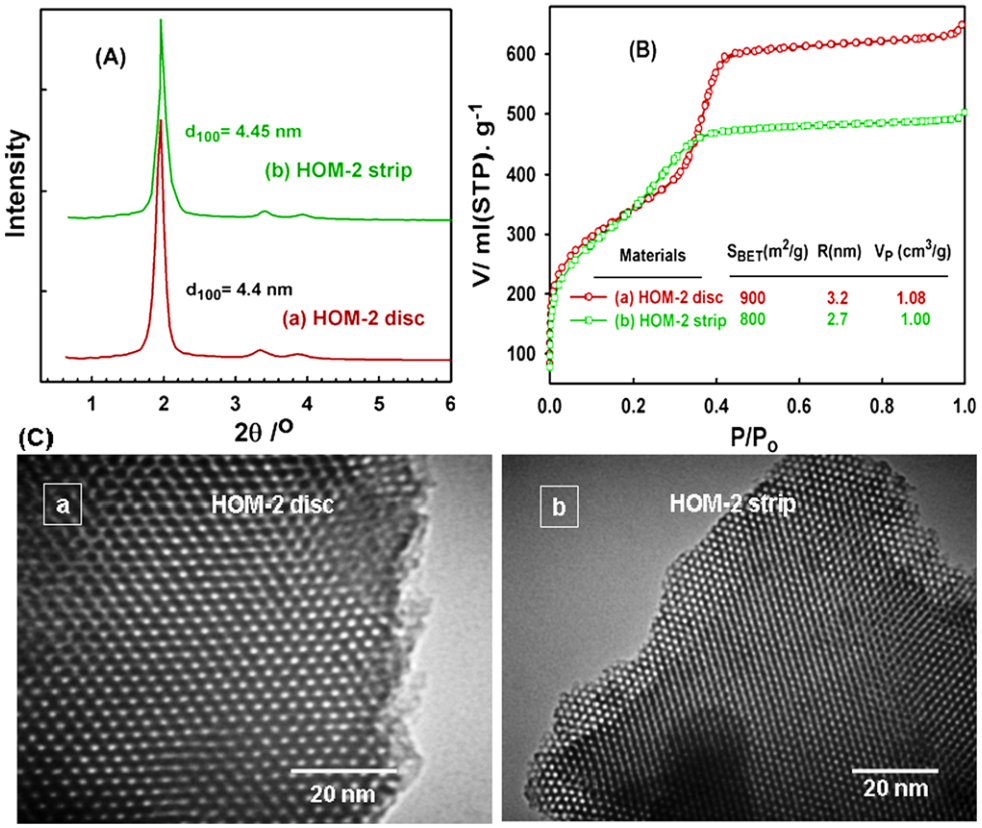

Figure 2 XRD patterns (**A**), N_2 adsorption/desorption isotherms at 77 K (**B**), and TEM micrographs (**C**) of hexagonal HOM-2 silica membrane disc (**a**) and azo-probe strip (**b**), respectively. Insert lists (**B**) mesopore size (R) and volume (V_p), and surface area (S_{BET})

sion of the organic moieties, to some extent, into the hexagonal mesopore without significant influence on the uniformly-sized structures, as evidenced from XRD and TEM profiles (Figs. 2A, C). The decrease in the surface area and pore volume with the fictionalization of HOM-2 silica provided further evidence for the embedding of the organic moieties inside the mesopore; however, such inner incorporation onto the pore does not exclude the possible coexistence of the embedding of the organic moieties onto the outer pore surfaces. TEM images show uniform arrangement pores and continuous arrays along all directions of the hexagonal geometry even after incorporating of the azo-probe chromophore moieties (Fig. 2C). Our findings indicated that the direct interaction between the azo-probe molecule and silica disc (Scheme 2) was sufficient to load the hydrophobic probe into the rigid condensed pore surfaces with retention of the ordered structures, leading to high flux and Co(II) ion-transport during the naked-eye detection process.

Furthermore, our sensor design not only led to strongly bound azo-probe with higher loading capacity onto the pore surfaces, but also enhanced the accessibility of the azo-probe to Co(II) ions without any increase in kinetic hindrance compared with that of an indirect grafting process (El-Safty et al. 2006). In fact, the ability to achieve flexibility on the specific activity of the electron acceptor/donor strength of the molecular probe might lead to easily generate and transduce an optical color signal as a response to the probe-Co(II) analyte binding events. The XPS patterns of Co 2p spectra show two main peaks of $2p_{1/2}$ and $2p_{3/2}$ at 766.4 and 781.2 eV, which assigned to the Co(II) ions in the cobalt compounds. Although, the binding energy of Co $2p_{3/2}$ peak was shifted around 1.2 eV to higher values compared to that of CoOOH (780.0 eV) (Moulder et al. 1992). This blue shift in the $2p_{3/2}$ peak could be assigned to the existence of the Co(II) ions inside the HOM mesopores during the detection process. The XPS results, in general, mainly indicated the dispersion of the dominant Co(II) ions in intrinsic complex formation into the pore wall surfaces of HOM strip. Moreover, the well resolved extra satellite peaks (at higher binding energy of the main line in both edges) of the Co 2p spectra (Fig. 3) indicated the existence of Co(II) ions. Moreover, the satellite peak (790.5 eV, see the single components) and the $2p_{3/2}$-$2p_{1/2}$ doublet separation ($\Delta = 14.8$ eV) were clearly indicated the binding of the Co(II) ions with azo-dye probes.

3.2 Hexagonal Co(II) ion-sensing strip procedure

During the Co(II) ion sensing studies, the effects of experimental sensing factors such as, the pH, temperature, sample volume, response time (R_t), and the critical thickness of the probe-modified HOM monoliths were studied to optimize batch equilibration conditions for a quick visual detection

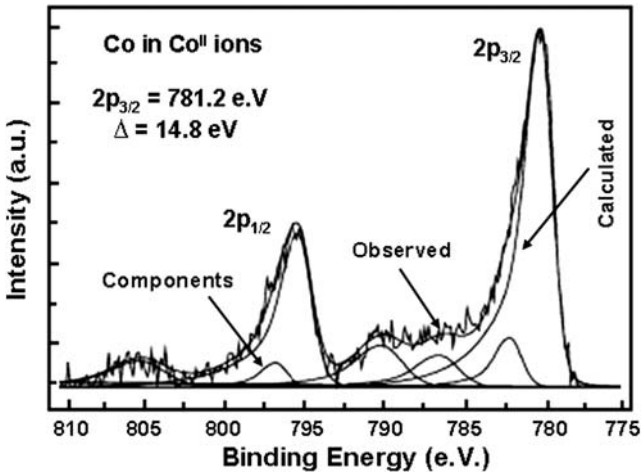

Figure 3 XPS patterns of the Co 2p spectra and a deconvolution to a single component of the spectra for the HOM-2 sensor strip after detection of 0.1 ppm Co(II) ions

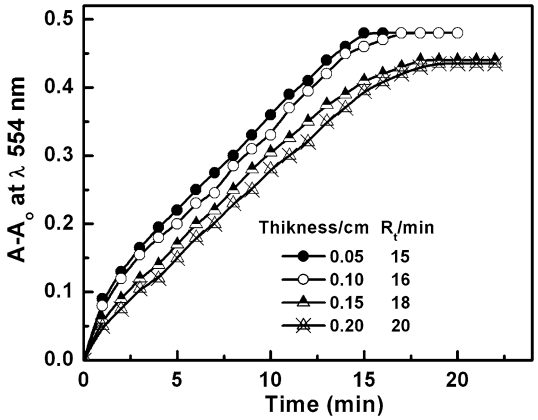

Figure 5 Kinetic variation of the absorption signal response with respect to the thickness of hexagonal monolithic strip during the recognition of [75 ppb] Co(II) ions at pH 5.5, at temperature 25 °C and at 20 ml of total volume. The A and A_0 are the absorption signal responses of the strip after and before (blank) the addition of Co(II) ion

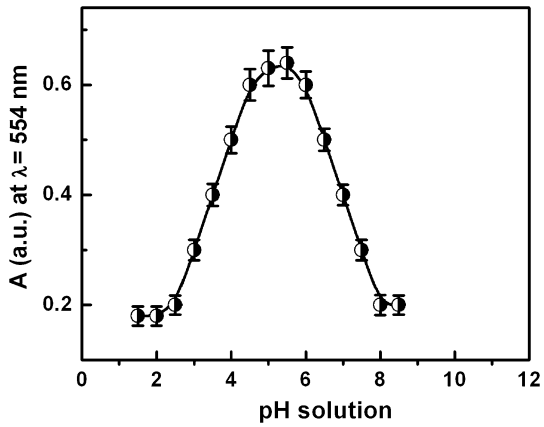

Figure 4 pH dependent response profile observed for HOM-2 hexagonal monolithic strip, when equilibrated individually at different pH conditions, with [75 ppb] Co(II) ion at temperature 25 °C, 0.05 cm thickness and at $R_t \geq 15$ min

of Co(II) ions. The efficiency of Co(II) ion-sensor was influenced by the pH solution. The reflectance spectra of the [Co-probe]$^{n+}$ complex at $\lambda = 554$ nm was carefully monitored over a wide range of pH solutions (Fig. 4). The hexagonal strip was sensitive in terms of their optical "color intensity" and signal response for Co(II) ions at pH 5.0–6.0.

The quantification procedure of Co(II) ion-sensing with HOM-2 strip studied after equilibration time, namely response time (R_t), in which the prominent color change and signal saturation in the strip reflectance spectra were achieved (Fig. 5). The kinetic time-response of the [Co-probe]$^{n+}$ complex formation was studied by continuously monitoring the absorption spectra (Fig. 5) and the color change of the sensors after addition of Co(II) ion as a function of time at various strip thickness. The result show that charge transfer between the Co(II) and azo-probe was accomplished after 15 min. In turn, the increase of the thickness of hexagonal strips makes the Co(II) ion-permeability through the dense probe molecular assemblies to the active binding sites more difficult. Results also indicated that the thicker strips show difficulty in the distinguishable color changes during the detection the trace Co(II) analytes.

3.3 Colorimetric recognition of azo-probe receptor in solution

For the visual detection of Co(II) ion in an aqueous phase, we carried out sensing experiments of Co(II) ion using the azo-probe molecular receptor in solution (Fig. 6). The absorption spectrum of the azo-probe in the ethanol phase shows a maximum absorption at λ_{max} of 390 nm (Fig. 6A). The Co(II) quantification experiments were carried out on a quartz flask with a total volume of 20 mL. The Co(II) aliquots were injected from a 10 mM aqueous stock solution into the flask containing a mixture solution of 30 μM azo-probe and pH 5.5 at constant temperature of 25 °C. The addition of specific amounts of Co(II) ions to the azo-probe induced the changes in the probe chromophore absorption spectrum to λ_{max} of 560 nm. However, the binding of Co(II) ions with azo-probe led to the formation of the chelate [Co-(probe)$_2$]$^{n+}$ complex (Scheme 1) (Lei et al. 2006). In general, the optically visible and spectral intense transitions were observed when the aqueous medium was maintained within the pH of 5.5, at signal response-time ($R_t \geq 15$ minute), Fig. 6. The responsible for naked-eye detection is clearly observed in the range of 0.2–3.0 ppm, as evidenced by the color change from yellow to a deep-violet (Fig. 6B). On the other hand, the stoichiometric Co(II)-probe reaction was revealed from Job's plot in solution under our experimental conditions. Results indicated a 1:1 binding for probe with Co(II) ion (Scheme 1 and 2).

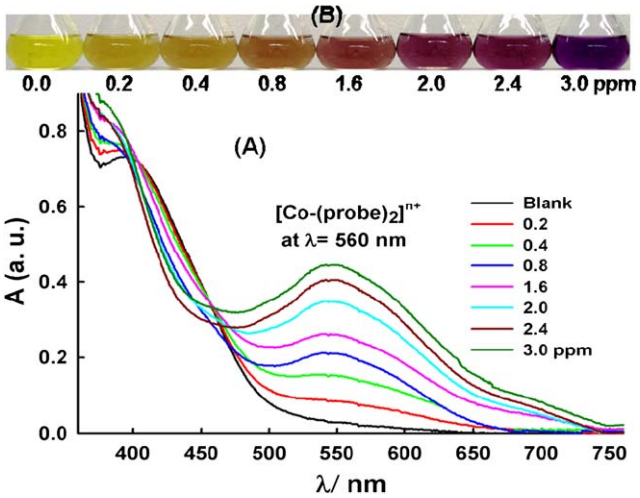

Figure 6 Changes in the UV-vis absorption spectra (**A**) and the colorimetric response profile (**B**) of 15 μM azo-probe solutions in ethanol medium upon titration with standardized Co(II) ions, at temperature 25 °C. The pH of the medium was adjusted to 5.5 for optimum spectral and colorimetric isolation. A constant stay time of 15 minutes was maintained for stable color development for all solutions with 20 ml volume

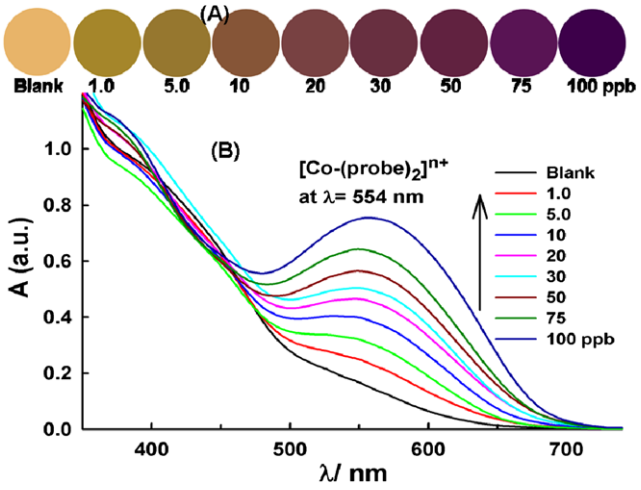

Figure 7 Colour transition map (**A**) and reflectance spectra (**B**) observed for hexagonal strips with increasing concentrations of Co(II) ions at pH of 5.5, total volume of 20 ml, temperature 25 °C, and equilibrating time for 15 minutes, respectively. The thickness of the strip monoliths was maintained at 0.05 cm to optimize the colorimetric and spectral responses

3.4 Optical ion-sensing monolithic strips

The design of hexagonal azo-probe monolithic strip provided a high degree of Co(II)-to-probe binding affinity leading to high sensitivity and stability sensing system under our simple sensing procedure, pH 5.5, temperature 25 °C, volume 25 ml, and a 0.05 cm thick (Fig. 7). Moreover, the design-made nanosensors with highly physical and textural properties could be used as efficient and simple preconcentrators with simultaneously visual inspection "naked-eye" of Co(II) ions. The hexagonal strip shows evidence of the visual detection over a wide, adjustable range between 1.0 ppb to 0.1 ppm (Fig. 7A). The color transition corresponding to the formation of $[\text{Co-(probe)}_2]^{n+}$ complex (Scheme 2) provided a simple procedure for sensitive and selective detections of Co(II) ions by naked-eye without the need for sophisticated instruments (Fig. 7A) (Nicole et al. 2004). The color intensity and homogeneity increased with increasing Co(II) ion concentration (El-Safty et al. 2008a, 2008b, 2008c). The colorimetric quantification of hexagonal strip for Co(II) ion-sensing over a wide range of concentration was also investigated by monitoring the UV/Vis reflectance spectra. The colorimetric determination of Co(II) ions was revealed in the detection range of 1.0 ppb to 0.1 ppm (Fig. 7B). The spectra of the azo-probe modified hexagonal strip at λ_{max} of 390 nm exhibited a bathochromic shift to 554 nm by addition of Co(II) ions, indicating the formation of the charge-transfer $[\text{Co-(probe)}_2]^{n+}$ complex. In addition, the stability constant ($\log K_s$) of the formed $[\text{Co-(probe)}_2]^{n+}$ complex into the nanosensors at pH 5.5 was estimated as 12.9, according to the following equation (2) (Winker et al. 1998):

$$\log K_s = [\text{ML}]_S / [\text{L}]_S * [\text{M}] \quad (2)$$

where [M] refers to the concentration of Co(II) ions in solution that have not reacted with the azo-probe chelating agent, [L] represents not only the concentration of free azo-probe ligand but also all concentrations of azo-probe not bound to the Co(II) ion, and the subscript S refers to the total concentration and the species in the solid phase (El-Safty et al. 2007a). Results form the binding constant of $[\text{Co-(probe)}_2]^{n+}$ complex indicated that sulfur-, oxygen-, and nitrogen-chelating groups of azo-probe ligand tightly bind to Co(II) ions in the typically octahedral $[\text{Co-(probe)}_2]^{n+}$ complex formation at the pH solution of 5.5 (Scheme 2).

3.5 Hexagonal ion reversible sensor strips

The reusability and reproducibility of the hexagonal strip were reveled after multiple regeneration/reuse cycles. In such treatment procedure, we used the stripping agent CH_3COO^- anion with 0.2 M concentration to effectively remove the Co(II) ions (i.e. decomplexation) after a complete detection process (El-Safty et al. 2006). After several times of the liquid-exchange process, the sensor was collected and washed by deionized H_2O. The UV/Vis reflectance spectrum of azo-dye modified monoliths at $\lambda = 390$ nm was measured and revealed no change in the signal intensity, indicating no potential leaching of azo probe modified HOM-2 during the regeneration process. Results observed that the decomplexation process of the Co(II) analyte could be carried out up to 6 repeated cycles, without significant loss in

the sensing efficiency of the strip, as we previously reported with the cage sensor (El-Safty et al. 2006). However, as a consequence of the regeneration/reuse cycles, the stripping agent mainly affected on the deactivation behavior of the specific activity of the probe binding affinity, as evidenced from the slight decrease in the sensitivity of the Co(II) ion sensor utilities.

3.6 Calibration of the monolithic strips

The calibration plot of the hexagonal strip during Co(II) ion-sensing was determined. However, the quality of the sensor strip is necessary to ensure both accuracy and precision of the Co(II) ion sensing systems. Several quantification measurements (≥10 times) were carried out using wide-range concentrations (1.6×10^{-8} to 1.7×10^{-6} M) of the standard "well-known" solutions of Co(II) ions at the specific sensing conditions and in the absence of both cation and anion interferences (Fig. 8, solid line). In general, the calibration methods show a linear correlation at low concentration ranges of Co(II) analyte ions (Fig. 8). The linear curves indicated that the Co(II) analyte can be detected with highest sensitivity. In fact, the standard deviation for the analysis of Co(II) ions using hexagonal strip was of 0.6%, as evidenced for the fitting plot of the calibration graphs (Fig. 8, inserts). The detection (L_D) and quantification (L_Q) limits of Co(II) ions using the hexagonal strip were estimated to be 0.88 ppb and 2.9 ppb, respectively, according to the following equation (3) (Christian 2003):

$$(L_D) \quad \text{or} \quad (L_Q) = kS_b/m \tag{3}$$

where, S_b and m are the standard deviation and the slope of the linear calibration graph (Fig. 8, inserts), the constant k is equal to 3 and 10 in the case of the determination of L_D and L_Q, respectively.

3.7 Hexagonal ion selective sensor strips

An important issue related to chemical sensor feasibility is the selectivity factor in which high range of linearity was required for the practical determination of Co(II) ions over multi-component analytes using the azo-probe under our specific sensing procedures. We firstly studied the binding affinity of azo-probe towards Co(II) target analyte in solution phase. However, a series of transition and group I and II metal ions was added to the sensing system containing 3.0 ppm Co(II) at pH 5.5 and at 25 °C (see their levels of tolerances in Table 1). The binding affinity of azo-probe molecule for Co(II) over a series of transition and group I and II metal ions (Li^+, Na^+, K^+, Mg^{2+}, Ca^{2+}, Cu^{2+}, Zn^{2+}, Cd^{2+}, Mn^{2+}, Ni^{2+}, Fe^{3+}, and Hg^{2+}), at pH 5.5 was investigated. The time frame required for a complete color development

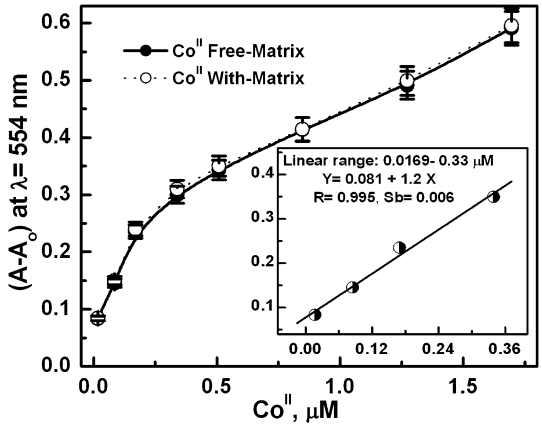

Figure 8 Calibration plot for hexagonal sensor strip of the spectral absorbance measured at λ_{max} of 554 nm with different Co(II) concentrations (*solid line*). *Insert*, the *linear fit line* at the linear concentration range (0.0169–0.33 μM) before saturation of the calibration plots for ordered sensor strip of the spectral absorbance measured at λ_{max} of 554 nm with different Co(II) concentrations. The *dotted line* represented the calibration plot of the Co(II) ions in the presence of the active interfering species at the same sensing conditions of pH 5.5, temperature 25 °C, 0.05 cm thickness, R_t 15 min and volume 20 ml. The sensing analytical data for the Co(II) ions for both cases were recorded with ten replicate analyses. The error bars denote a relative standard deviation of >0.55%

with stable signal intensity was estimated by kinetic measurements to be about 15 minutes. The Co(II) ion-selectivity studies revealed no spectral interferences from alkali-earth metals ion even >3.5 ppm. However, significant interferences were observed from transition metal ions especially from Mn^{2+}, Cu^{2+}, Ni^{2+}, Hg^{2+} and Zn^{2+}, which subsequently produced a positive signal response, when their concentrations in the solution exceeds beyond 0.1 ppm (see Table 1). The solution chemistry of azo-probe revealed a selective behavior of Co(II) ion by using suppressing agents for first row transition metal ions, such as 2% NaCN (or) 0.3 mM citrate and tartrate mixture, under our physiological pH conditions. Significantly, the addition of various types of surfactants and anion species had no interference effects for Co(II) ion-selective system in solution.

Second, by applying the hexagonal strip, results also show the efficient Co(II) ion-selective sensor strip with high tolerable level of interfering matrix concentrations (Table 2). Indeed, high response speed and confidence in the recognition of Co(II) analytes from samples containing of chemically complex matrices were achieved by using these membrane-disc strips at our specific sensing conditions (pH, time ≥ R_t, 0.05 cm thick, solution volume of 25 ml, and temperature of 25 °C). The calibration plot (Fig. 8, dotted line) of Co(II) analyte in the presence of the matrix species shows evidence of the significant correlation of the recognition sensing procedure of Co(II) ion by the fabricated hexagonal strips. With addition of transition metal ions, the azo-probe modified sensor exhibited a good tolerance for major and ac-

Table 2 Tolerance concentration for interfering matrix species during recognition of [0.1 ppm] Co(II) ions by azo-probe modified hexagonal strip

Tolerance limit for common electrolyte species (ppm) with sensor 4											
NaCl	NaBr	KNO_3	SO_4^{2-}	F^-	PO_4^{3-}	CO_3^{2-}	NO^{2-}	ClO_4^-	IO_3^-	SCN^-	SO_3^{2-}
6750	1560	7550	3340	375	180	250	300	761	50	98	250
Tolerance limit for foreign cations (ppm)											
Sn^{2+}	Fe^{3+}	Mn^{2+}	Hg^{2+}	Ni^{2+}	Zn^{2+}	Cu^{2+}	Ir^{3+}	Cr^{6+}	Sb^{3+}	Al^{3+}	Bi^{3+}
4.0	3.5	2.5[a]	2.0[a]	1.8[a]	1.5[a]	2.2[a]	3.5	4.5	4.0	3.5	3.8
Tolerance limit for surfactants and complexing agents (μM)											
CTAB	TAAC	TEAC	DDAB	SDS	TX	Oxal.	Citr.	Tart.	Phth	Acet.	H.A
64	65	75	68	44	79	160	365	360	266	310	0.001

[a]Data obtained after using suppressing agents

Abbreviations: CTAC—Cetyltrimethyl ammonium bromide; DDAB— Dilauryl dimethyl ammonium bromide; TAAC—Tetraamyl ammonium chloride; TEAC—Tetraethyl ammonium chloride; SDS—Sodium dodecyl sulfate; TX—Triton X-100; Oxal.—Oxalate; Citr.—Citrate; Tart.—Tartrate; Phth—Phthalate, Acet.—Acetate, H.A—Humic acid

tive foreign cations (Table 2). However, the solution chemistry of azo-probe revealed a selective behavior of the Co(II) ion by using suppressing agents (Table 1). In fact, by using the hexagonal strip, the heavy metal ions such as, Al^{3+}, Bi^{3+}, Cr^{6+}, La^{3+}, Ir^{3+}, Sn^{2+} and Sb^{3+} did not interfere in the Co(II) ion-sensing system, even with a tolerable concentration $\leq$4 ppm. The Cu^{2+}, Ni^{2+}, Hg^{2+}, and Zn^{2+} showed interference, which was eliminated by using 0.2 mM thiosulphate and thiocyanide. These results indicated that the behavior of azo-probe solid strip with the Co(II) analyte and its matrix environments showed conspicuous divergence from their solution chemistry. Such finding might indicate that the orientation and arrangement of the probe molecular assemblies mounted onto HOM-2 solid carriers with open-pore arrays, high surface areas, and high pore volumes allowed stable thermodynamic binding of Co(II)-probe chelates (El-Safty et al. 2008a, 2008b, 2008c).

3.8 Hexagonal strip in synthetic wastewater samples

The high degree of Co(II) ion selectivity by using hexagonal strip makes it potentially useful for monitoring the trace level of concentration of Co(II) ions in real-life samples such as a wastewater. For this study, simulated multicomponent solution containing Fe^{3+}, Cd^{2+} (50 mg/L); Zn^{2+}, Cu^{2+}, Ni^{2+} (10 mg/L); Sb^{3+}, Hg^{2+} (50 mg/L); Ca^{2+}, Mg^{2+} (100 mg/L); along with PO_4^{3-}, SO_4^{2-}, SO_3^{2-} (100 mg/L); CH_3COO^-, Cl^- (100 mg/L) and NO_3^-, CO_3^{2-} (100 mg/L) samples were spiked to a standard solution of Co(II) 0.1 mg/L. Despite the addition of these effective disturbance species, particularly when these species are existed in multi-component system at a high concentration, the analytical data reveal that no significant effects of these spiked multicomponents in the selectivity of the developed nanosensors for Co(II) ions. The recognition of Co(II) ion was visualized by naked eye and quantitatively determined by UV spectra at $\lambda = 554$ nm. The quantification data of the Co(II) ion sample examined six times were fitted the calibration plot (Fig. 8, dotted line). The calibrated concentration of Co(II) ion in these multicomponent samples was 0.1 mg/L ($\pm$0.005) with confidence level of 98.5% and with relative standard deviation of 2%. Such results indicated that the hexagonal strip can be highly applicable for environmental cleanup of toxic heavy metal ions.

3.9 Stability of the hexagonal sensor strips

The actively long-term shelf-time of the strip efficiency makes the optical strip technologically promising. A long-term retention of the azo probe-modified monolithic sensors was examined under storage for several months (El-Safty et al. 2006). Despite the direct inclusion of the azo-dye probe into silica monoliths without use of the surface modifier, the developed sensors-based hexagonal nanostructure materials provided control over the potential leaching out of the chromophore upon the storage. Our results show that little changes in the optically colored density "absorption spectra" of probes were evident after storage for relatively longer times (i.e. $\geq$4 months). The relatively high storage stability, in principle, indicated the effect of the use of hexagonal nanostructures with their open pores and with modified-azo probe assembly in the fractal networks in terms of actively long-term shelf-time of the sensors. Compared with chemosensor design using surface modification, in which strong electrostatic interactions 'Coulombic-types' between the probe molecule and charged silica surfaces (El-Safty et al. 2006, 2007a, 2007b) were occurred, the stability under storage "shelf time" of this solid sensor design

is much higher than that sensor design based on physisorbing probe molecules. But one should bear in mind that the latter design provided higher flexibility on the specific activity of the electron acceptor/donor strength of the molecular probe than that immobilization method using surface modifiers, leading to easily generate and transduce an optical color signal and a fast kinetic azo probe-Co(II) binding responses. In general, our sensor deign using direct inclusion of azo probes provided adequate sensing design in terms of sensitivity, selectivity, reproducibility and acceptable degree, to high extent, of stability and shelf time.

4 Conclusion

Hexagonal sensor strip for sensitive, selective and high response detection was successfully fabricated and tested. Key to our development design of sensor monoliths is that although the azo-dye receptor was successfully used for a Co(II) ion-sensing recognition in solution up to $\sim 10^{-7}$ M, our strip enabled to create ion-sensitive responses with revisable, selective and sensitive recognitions of a wide range of detectable Co(II) ions down to sub-nanomolar ($\sim 15 \times 10^{-9}$ M) in rapid sensing responses (in the order of minutes). Due to the probe accommodation into nanoscale HOM monoliths, the intrinsic property and functionality of the probe receptor in terms of stability, selectivity, sensitivity and binding response kinetics were significantly changed with its respect to the physical properties of the hexagonal HOM-2 monoliths. The current studies emphasized that the use of hexagonal HOM-2 monoliths as probe templates had profound the sensing advantages over the liquid colorimetric determination using azo-dye receptor. Considering the environmental factors, the solid-state probe strips were solvent-free systems and had the capacity to serve as ion preconcentrators with complete reversibility and reusability. These features of the probe-design nanosensors might lead to overcome the disposal problems, which normally associated with the liquid probe systems. In addition, the behavior of solid-probe strip with the Co(II) analytes and its matrix environment showed conspicuous divergence from its solution chemistry. The specific utility of nanosensor was interesting on its application as an ion-sensing tool.

References

Alexandersson, R.: Arch. Environ. Health **43**, 299–303 (1988)

Anastas, P.T.: Crit. Rev. Anal. Chem. **29**, 167–175 (1999)

Angerer, J., Heinrich-Ramm, R., Lehnert, G.J.: Environ. Anal. Chem. **35**, 81–88 (1989)

Benkhadda, K., Infante, H.G., Ivanova, E., Adams, F.: J. Anal. Atom. Spectrom. **15**, 429–434 (2000)

Buhlmann, P., Pretsch, E., Bakker, E.: Chem. Rev. **98**, 1593–1687 (1998)

Burns, D.T., Kheawpinting, S.: Anal. Chem. Acta **162**(1), 437–442 (1984)

Carringto, N.A., Xue, Z.-L.: Acc. Chem. Res. **40**, 343–350 (2007)

Christensen, J.M., Poulsen, O.M.: Sci. Total Environ. **150**(1–3), 95–104 (1994)

Christian, G.D.: Analytical Chemistry, 6th edn. Wiley, New York (2003)

Comes, M., Marcos, M.D., Sancenon, F., Soto, J., Villaescusa, L., Amoros, A., Beltran, P.D.: Adv. Mater. **16**, 1783 (2004)

Dadfarnia, S, Jafarzadeh, M.H.: Microchem. J. **63**(2), 226–234 (1999)

De Boeck, M., Kirsch-Volders, M., Lison, D.: Mutat. Res. **533**, 135–152 (2003)

Desacalzo, A.B., Rurack, Weisshoff, K.H., Manez, R.M., Marcos, M.D., Amoros, P., Hoffmann, K., Soto, J.J.: Am. Chem. Soc. **127**, 184 (2005)

Dominique, L.: Handbook on the Toxicology of Metals; 3rd edn, pp. 511–528 (2007)

El-Safty, S.A.: J. Colloid Interface Sci. **260**, 184–194 (2003)

El-Safty, S.A., Evans, J.: J. Mater. Chem. **12**, 117–123 (2002)

El-Safty, S.A., Hanaoka, T.: Adv. Mater. **15**(22), 1893–1899 (2003)

El-Safty, S.A., Hanaoka, T., Mizukami, F.: Adv. Mater. **17**(1), 47–53 (2005)

El-Safty, S.A., Balaji, T., Matsunaga, H., Hanaoka, T., Mizukami, F.: Angew. Chem. Int. Ed. **45**, 7202 (2006)

El-Safty, S.A., Ismail, A., Matsunaga, H., Mizukami, F.: Chem. Eur. J. **13**, 9245 (2007a)

El-Safty, S.A., Prabhakaran, D., Ismail, A., Matsunaga, H., Mizukami, F.: Adv. Funct. Mater. **17**, 3731 (2007b)

El-Safty, S.A., Ismail, A.A., Matsunaga, H., Mizukami, F.: J. Phys. Chem. **112**, 4825–4835 (2008a)

El-Safty, S.A., Ismail, A.A., Matsunaga, H., Hanaoka, T., Mizukami, F.: Adv. Funct. Mater. **18**, 1485–1500 (2008b)

El-Safty, S.A., Prabhakaran, D., Ismail, A.A., Matsunaga, H., Mizukami, F.: Chem. Mater. **20**, 2644–2654 (2008c)

Elinder, C.G.: Toxicol. Environ. Chem. **7**, 251–256 (1984)

Haga, Y., Clyne, N., Hoffman-Bang, C., Pehrsson, S.K., Ryden, L.: Trace Elem. Electrolytes **13**(2), 69–74 (1996)

Hamilton, E.I.: Sci. Total Environ. **150**(1–3), 7–39 (1994)

Hartung, M., Schaller, K.H., Brand, E.: Int. Arch. Occup. Environ. Health **50**, 53–57 (1982)

Hursthouse, A.S.: J. Environ. Monit. **3**(1), 29–60 (2001)

Imray, P., Landley, A.: Soil **1**, 45 (1999)

Jensen, A.A., Tüchsen, F.: CRC Crit. Rev. Toxicol. **20**, 427–437 (1990)

Keith, L.H., Gron, L.U.J., Young, L.: Chem. Rev. **107**, 2695–2708 (2007)

Lee, J.-S., Han, M.S., Mirkin, C.A.: Angew. Chem., Int. Ed. **46**, 4093 (2007)

Lei, B., Li, B., Zhang, H., Lu, S., Zheng, Z., Li, W., Wang, Y.: Adv. Funct. Mater. **16**, 1883 (2006)

Lison, D., De Boeck, M., Verougstraete, V., Kirsch-Volders, M.: Occup. Environ. Med. **58**, 619–625 (2001)

Malcik, N., Oktar, O., Ozser, M.E., Caglar, P., Bushby, L., Vaughan, A., Kuswandi, B., Narayanaswamy, R.: Sens. Actuators B **53**, 211–221 (1998)

Mennè, T., Nieboer, E.: Endeav. New Ser. **13**, 117–122 (1989)

Morgan, L.G.: J. Soc. Occup. Med. **33**, 181–186 (1983)

Moulder, J.F., Stickle, W.F., Sool, P.E., Bomber, K.D.: Handbook of X-ray Photoelectron Spectroscopy. Perkin-Elmer, Eden Prairie (1992)

Nagpal, N.K.: Water Quality Guidelines for Cobalt. Victoria (2004)

Nam, J.-M., Thaxton, C.S., Mirkin, C.A.: Science **301**, 1884 (2003)

Nicole, L., Boissiere, C., Grosso, D., Hesemann, P., Moreau, J., Sanchez, C.: Chem. Commun. 2312–2313 (2004)

Niessner, R.: Trends Anal. Chem. **10**, 310 (1991)

Oehme, I., Wolfbeis, O.S.: Mikrochim. Acta **126**, 177 (1997)
Pal, A., Ghosh Paul, S., Paul, A.K.: Bioresour. Technol. **97**, 1253–1258 (2006)
Pretsch, E., Buhlmann, P., Bakker, E.: Chem. Rev. **97**, 3083–3132 (1997)
Ros-Lis, J.V., Marcos, M.D., Mártinez-Mánez, R., Rurack, K., Soto, J.: Angew. Chem. Int. Ed. **44**, 4405 (2005)
Safavi, A., Shams, E.: Talanta **51**, 1117–1123 (2000)
Simpson, N.J.K.: Solid Phase Extraction, Principle, Techniques and Applications. Marcel Dekker, New York (2000)
Singh, A.K., Mehtab, S., Saxena, P.: Sens. Actuators B **120**, 455–461 (2007)
Umemura, T., Hotta, H., Abe, T., Takahashi, Y., Takiguchi, H., Uehara, M., Odake, T., Tsunoda, K.: Anal. Chem. **78**, 7511 (2006)
Vega, M., Van der Berg, C.M.G.: Anal. Chem. **69**, 874–881 (1997)
Winker, J.D., Bowen, C.M., Michelete, V.: J. Am. Chem. Soc. **120**, 3237 (1998)
Wolfbeis, O.S.: J. Mater. Chem. **15**, 2657 (2005)
Yang, R., Wang, K., Long, L., Xiao, D., Yang, X., Tan, W.: Anal. Chem. **74**, 1088–1096 (2002)
Zhang, C., Suslick, K.S.: J. Am. Chem. Soc. **127**, 11548 (2005)